

# Performance Evaluation of Bridgeless PFC Boost Rectifiers

Laszlo Huber, Yungtaek Jang, and Milan M. Jovanović

Delta Products Corporation  
 Power Electronics Laboratory  
 P.O. Box 12173  
 5101 Davis Drive  
 RTP, NC 27709, U.S.A.

**Abstract** - In this paper, a systematic review of bridgeless PFC boost rectifiers, also called dual boost PFC rectifiers, is presented. Performance comparison between the conventional PFC boost rectifier and a representative member of the bridgeless PFC boost rectifier family is performed. Design considerations and experimental results in both CCM and DCM/CCM boundary operations are provided.

## I. INTRODUCTION

To meet the challenges of ever-increasing power densities of today's ac/dc power supplies, designers are continuously looking for opportunities to maximize the power-supply efficiency, minimize its component count, and reduce the size of components. Recently, in an effort to further improve the performance of the front-end PFC rectifier, many power supply manufacturers and some semiconductor companies have started looking into bridgeless PFC circuit topologies. Generally, the bridgeless PFC topologies, also referred to as dual boost PFC rectifiers, may reduce the conduction loss by reducing the number of semiconductor components in the line-current path.

So far, a number of bridgeless PFC boost rectifier implementations and their variations have been proposed [1]-[15]. In this paper, a systematic review of the bridgeless PFC boost rectifier implementations that have received the most attention is presented. Performance comparison between the

conventional PFC boost rectifier and a representative member of the bridgeless PFC boost rectifier family is performed. Design considerations and experimental results in both CCM and DCM/CCM boundary operations are provided.

## II. REVIEW OF BRIDGELESS PFC BOOST RECTIFIERS

The basic topology of the bridgeless PFC boost rectifier [1]-[8] is shown in Fig. 1. Compared to the conventional PFC boost rectifier, shown in Fig. 2, one diode is eliminated from the line-current path, so that the line current simultaneously flows through only two semiconductors, as shown in Fig. 3, resulting in reduced conduction losses. However, the bridgeless PFC boost rectifier in Fig. 1 has significantly larger common-mode noise than the conventional PFC boost rectifier [13]-[15]. In fact, in the conventional PFC boost rectifier, the output ground is always connected to the ac source through the full-bridge rectifier (slow-recovery diodes  $D_3$  and  $D_4$  in Fig. 2); whereas, in the bridgeless PFC boost rectifier in Fig. 1, the output ground is connected to the ac source only during a positive half-line cycle, through the body diode of switch  $S_2$ , as shown in Fig. 3(a), while during a negative half-line cycle the output ground is pulsating relative to the ac source with a high frequency (HF) and with an amplitude equal to the output voltage. This HF pulsating voltage source charges and discharges the equivalent parasitic capacitance between the output ground and the ac line ground, resulting in a significantly increased common-mode noise.

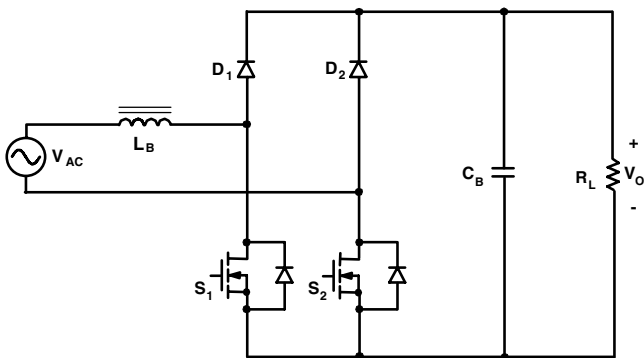


Fig. 1 Basic bridgeless PFC boost rectifier [1]

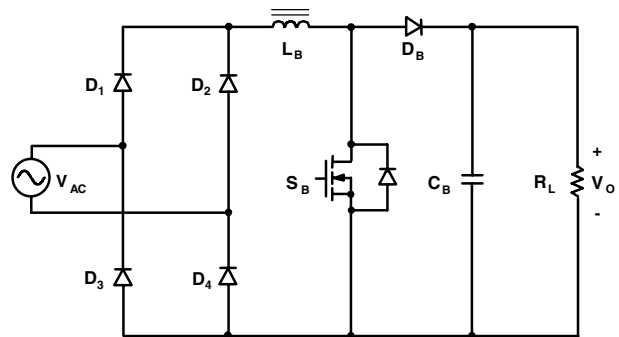
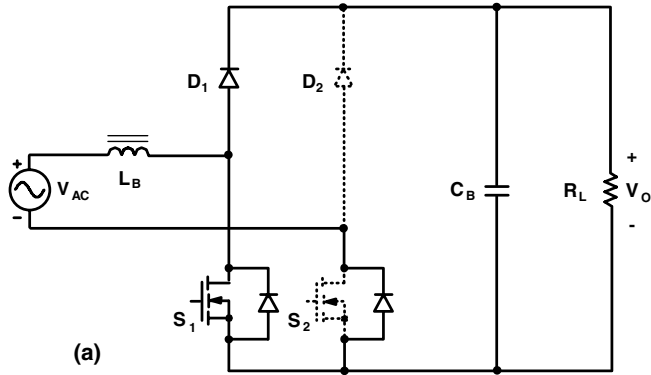
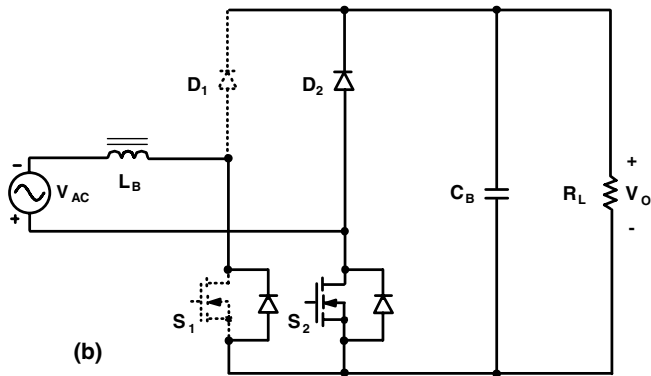


Fig. 2 Conventional PFC boost rectifier



(a)



(b)

Fig. 3 Basic bridgeless PFC boost rectifier in Fig. 1 during (a) positive half-line cycle and (b) negative half-line cycle

To reduce the common-mode noise of the bridgeless PFC boost rectifier in Fig. 1, i.e., to make it similar to that of the conventional PFC boost rectifier, the topology of the bridgeless PFC boost rectifier in Fig. 1 needs to be modified to always provide a low-frequency (LF) path between the ac source and the positive or negative terminal of the output.

In Figs. 4 and 6, the modification of the basic bridgeless PFC boost rectifier is implemented by adding two diodes,  $D_3$  and  $D_4$ . In addition, in Fig. 4, the common-source node of switches  $S_1$  and  $S_2$  is disconnected from the output ground. The circuit in Fig. 4 can be redrawn as shown in Fig 5, which is the bridgeless PFC boost rectifier with a bidirectional switch [3], [9]. It should be noted that in Fig. 5, diodes  $D_1$  and  $D_3$  are fast-recovery diodes, whereas, diodes  $D_2$  and  $D_4$  are slow-recovery diodes. During a positive half-line cycle, the ac source is connected to the output ground through slow-recovery diode  $D_4$ , and during a negative half-line cycle, the ac source is connected to the positive terminal of the output through slow-recovery diode  $D_2$ .

In Fig. 6, in addition to diodes  $D_3$  and  $D_4$ , which are slow-recovery diodes, a second inductor is also added, resulting in two dc/dc boost circuits, one for each half-line cycle [10], [11]. During a positive half-line cycle, the first dc/dc boost circuit,  $L_{B1}$ - $S_1$ - $D_1$ , is active through diode  $D_4$ , which connects the ac source to the output ground. During a negative half-

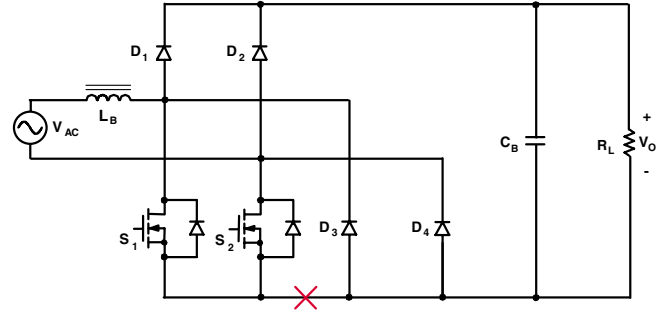


Fig. 4 Synthesis of bridgeless PFC boost rectifier with bidirectional switch from basic bridgeless PFC boost rectifier in Fig. 1

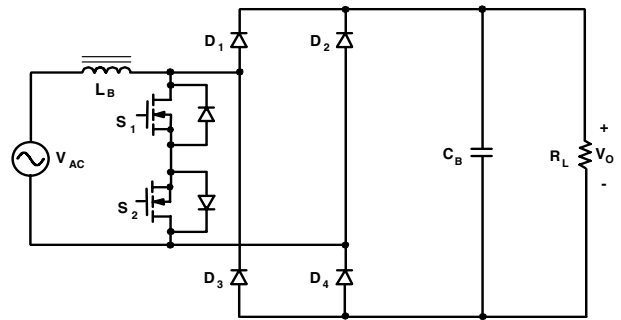


Fig. 5 Bridgeless PFC boost rectifier with bidirectional switch [3]

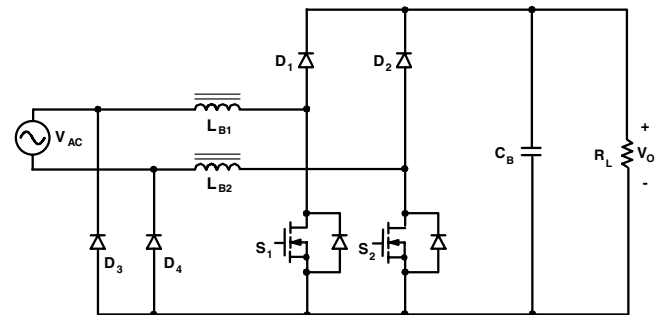


Fig. 6 Bridgeless PFC boost rectifier with two dc/dc boost circuits [10]

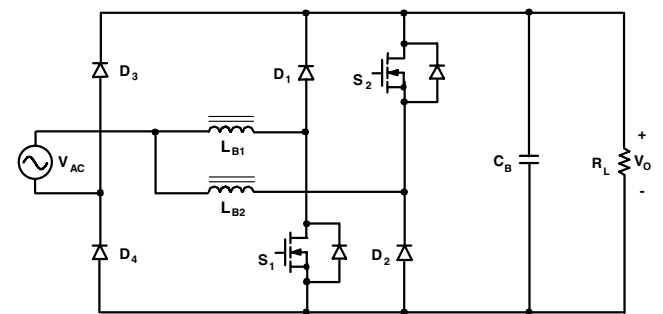


Fig. 7 Pseudo totem-pole bridgeless PFC boost rectifier [12]

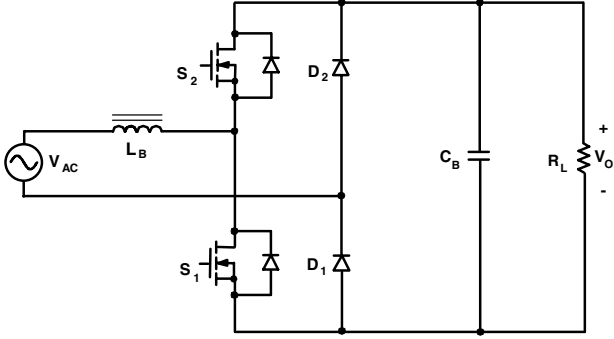


Fig. 8 Totem-pole bridgeless PFC boost rectifier [9]

line cycle, the second dc/dc boost circuit,  $L_{B2}$ - $S_2$ - $D_2$ , is active through diode  $D_3$ , which connects the ac source to the output ground.

It should be noted that switches  $S_1$  and  $S_2$ , in both bridgeless PFC boost rectifiers in Fig. 5 and Fig. 6, can be driven with the same PWM signal, which significantly simplifies the implementation of the control circuit. The drawback of the bridgeless PFC boost rectifier in Fig. 5 is that it requires an additional gate-drive transformer. The drawback of the bridgeless PFC boost rectifier in Fig. 6 is that it requires two inductors. However, it should also be noted that two inductors compared to a single inductor have better thermal performance.

Figure 7 shows a variation of the bridgeless PFC boost rectifier with two dc/dc boost circuits in Fig. 6 [12]. Because of the position of switches  $S_1$  and  $S_2$ , this topology is called pseudo totem-pole bridgeless PFC boost rectifier [12]. During a positive half-line cycle, dc/dc boost circuit  $L_{B1}$ - $S_1$ - $D_1$  is active through diode  $D_4$ , which connects the ac source to the output ground. During a negative half-line cycle, dc/dc boost circuit,  $L_{B2}$ - $S_2$ - $D_2$  is active through diode  $D_3$ , which connects the ac source to the positive terminal of the output. It should be noted that switches  $S_1$  and  $S_2$  in Fig. 7 cannot be driven with the same PWM signal. Furthermore, switch  $S_2$  requires an isolated gate drive. Therefore, the bridgeless PFC boost rectifier in Fig. 7 requires a more complex control and drive circuit and, consequently, it is less attractive for practical implementation than its counterpart in Fig. 6.

Finally, Fig. 8 shows a modification of the basic bridgeless PFC boost rectifier from Fig. 1 which is obtained by exchanging the position of diode  $D_1$  and switch  $S_2$  [9]. Because of the position of the two switches, the topology in Fig. 8 is called the totem-pole bridgeless PFC boost rectifier. It should be noted that diodes  $D_1$  and  $D_2$  are slow-recovery diodes. During a positive half-line cycle, the ac source is connected to the output ground through diode  $D_1$ , and during a negative half-line cycle, the ac source is connected to the positive terminal of the output through diode  $D_2$ . Because of the totem-pole arrangement of the switches, the bridgeless PFC boost rectifier in Fig. 8 can only work in DCM and at DCM/CCM boundary. In fact, the reverse-recovery performance of the body diodes of the switches makes CCM

operation of the bridgeless PFC boost rectifier in Fig. 8 impractical. Generally, the totem-pole bridgeless PFC boost rectifier in Fig. 8 requires a complex control and drive circuit. With the exception of the totem-pole bridgeless PFC boost rectifier in Fig. 8, the other bridgeless PFC boost rectifiers in Figs. 5-7 can operate in both CCM and DCM.

In Sections III and IV, as a representative member of the bridgeless PFC boost rectifier family, the bridgeless PFC boost rectifier in Fig. 6 is selected for performance comparison with the conventional PFC boost rectifier.

### III. DESIGN CONSIDERATIONS

Generally, the efficiency improvement of the bridgeless PFC boost rectifiers over the conventional PFC boost rectifier is predominantly limited by the on-resistance of the boost switches. The calculated efficiencies of both the conventional PFC boost rectifier (shown in Fig. 2) and the bridgeless PFC boost rectifier (shown in Fig. 6) operating in CCM and at the DCM/CCM boundary are shown in Figs. 9 and 10, respectively. The efficiency calculations include the conduction loss of the boost switches, boost diodes, full-bridge rectifier, boost inductor, EMI filter, and output capacitor, as well as the switching loss of the boost switches, the gate-drive losses, and the core loss of the boost inductors. It is assumed that in the efficiency calculations for the DCM/CCM boundary operation, the resonant interval, that is, the time it takes the voltage of the switch output capacitance to resonate down to its valley is negligible with respect to the switching period. For a fair comparison, it is assumed that the boost switch of the conventional PFC rectifier,  $S_B$  in Fig. 2, consists of two MOSFETs connected in parallel, while each switch of the bridgeless PFC boost rectifier,  $S_1$  and  $S_2$  in Fig. 6, comprises only one MOSFET. Similarly, the boost diode of the conventional PFC rectifier,  $D_B$  in Fig. 2, also consists of two diodes connected in parallel, while each diode of the bridgeless PFC boost rectifier,  $D_1$  and  $D_2$  in Fig. 6, comprises a single diode.

In the efficiency calculation for the CCM operation presented in Fig. 9, three different MOSFETs (SPP20N65C3 with  $R_{DSon} = 190 \text{ m}\Omega$ , IPP60R099CS with  $R_{DSon} = 99 \text{ m}\Omega$ , and IPW60R044CS with  $R_{DSon} = 44 \text{ m}\Omega$  from Infineon) are used for the boost switches. For the boost diodes and the input bridge rectifier, the STD08S60 (8-A, 600-V) SiC diode from Infineon and the D15XB60 (15-A, 600-V) full-bridge rectifier from Shindengen are used, respectively. Other power-stage components of the conventional and bridgeless PFC boost rectifiers are identical and considered to have identical losses.

As shown in Fig. 9, if the SPP20N65C3 MOSFET is used for the boost switches, efficiency of the bridgeless PFC boost rectifier is higher than that of the conventional PFC boost rectifier up to 400-W output power. If the IPP60R099CS or the IPW60R044CS MOSFET is used for the boost switches, the efficiency of the bridgeless PFC boost rectifier is higher than that of the conventional PFC boost rectifier over the

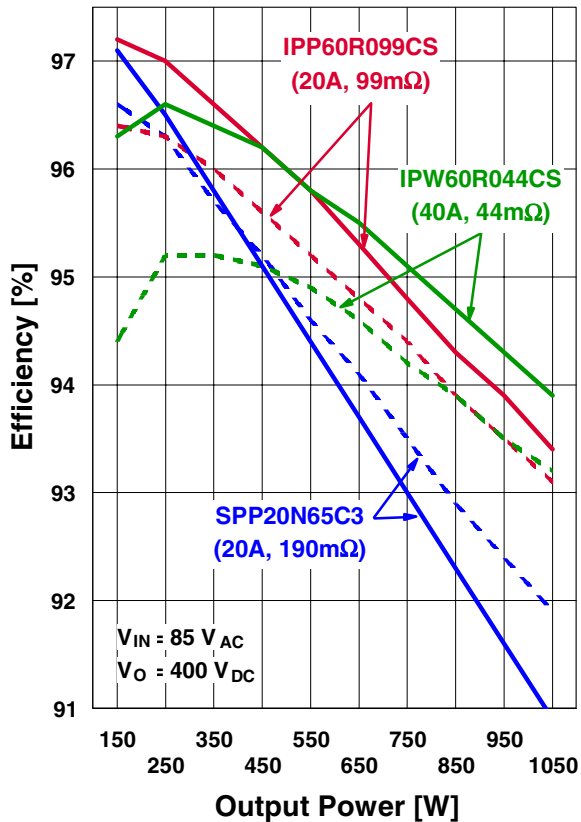


Fig. 9 Calculated efficiency of conventional PFC boost rectifier in Fig. 2 (dashed lines) and bridgeless PFC boost rectifier in Fig. 6 (solid lines) operating in CCM

entire calculated output power range. It should also be noted in Fig. 9 that the efficiency of the conventional PFC boost rectifier does not improve by replacing a small MOSFET (IPP60R099CS in TO-220 package) with a large MOSFET (IPW60R044CS in TO-247 package) below 1-kW output power, unlike the bridgeless PFC boost rectifier, which shows an efficiency improvement above 550-W output power when using a larger MOSFET. This is due to the increased switching losses. In fact, at low power levels, the efficiency of both the conventional and bridgeless PFC boost rectifiers is dominated by switching losses, whereas, at high power levels, the efficiency of both rectifiers is dominated by conduction losses. Since the conventional PFC boost rectifier employs both switches throughout the whole line cycle, the effective switch capacitance is twice as high as that of the bridgeless PFC boost rectifier, where each switch is employed only during one half of the line cycle, resulting in less overall switching losses.

It can be concluded from Fig. 9 that for high efficiency of the PFC boost rectifier operating in CCM, at output power levels above 600 W, the bridgeless PFC boost rectifier using the IPW60R044CS MOSFETs is the preferred solution; whereas, at output power levels below 400 W, the bridgeless PFC boost rectifier using the IPP60R099CS MOSFETs is

recommended. If switches with equal or higher  $R_{DSon}$  than that of the SPP20N65C3 MOSFET are employed, the conventional boost PFC circuit is the better choice.

In the efficiency calculation for the DCM/CCM boundary operation presented in Fig. 10, four different MOSFETs (SPP07N65C3 with  $R_{DSon} = 600 \text{ m}\Omega$ , SPP11N65C3 with  $R_{DSon} = 380 \text{ m}\Omega$ , IPP60R099CS with  $R_{DSon} = 99 \text{ m}\Omega$ , and IPW60R044CS with  $R_{DSon} = 44 \text{ m}\Omega$  from Infineon) are used for the boost switches. For the boost diodes and the input bridge rectifier, the ISL9R860P2 (8-A, 600-V) fast-recovery diode from Fairchild and the D15XB60 (15-A, 600-V) full-bridge rectifier from Shindengen are used, respectively. Again, the other power-stage components of the conventional and bridgeless PFC boost rectifiers are identical and, therefore, they are considered to have identical losses.

As shown in Fig. 10, for all MOSFETs except for the SPP07N65C3, which has the highest  $R_{DSon}$ , the efficiency of the bridgeless PFC boost rectifier is higher than that of the conventional PFC boost rectifier over the entire calculated output power range. The SPP11N65C3 MOSFET, which has an  $R_{DSon} = 380 \text{ m}\Omega$ , can be considered as the borderline to achieve an efficiency improvement by using the bridgeless PFC boost rectifier compared to the conventional boost PFC rectifier in the whole calculated output power range. It is also shown in Fig. 10 that at output power levels above approximately 200 W, the employment of the larger MOSFET

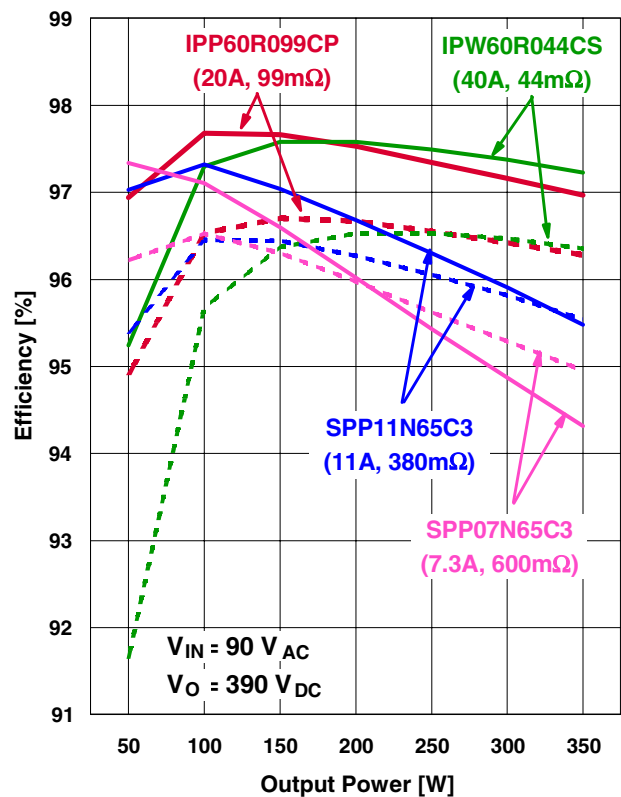


Fig. 10 Calculated efficiency of conventional PFC boost rectifier in Fig. 2 (dashed lines) and bridgeless PFC boost rectifier in Fig. 6 (solid lines) operating at DCM/CCM boundary

IPW60R044CS in TO-247 package results in the highest efficiency. However, the employment of the IPP60R099CS MOSFET yields the most uniform high efficiency in the whole calculated output power range. It can be concluded from Fig. 10 that the IPP60R099CS MOSFET used in the bridgeless PFC boost rectifier operating at the DCM/CCM boundary, exhibits an optimal balance between the conduction losses and the switching losses in the calculated output power range.

#### IV. EXPERIMENTAL RESULTS

A 750-W, constant switching frequency (110 kHz) CCM experimental circuit and a 300-W, variable switching frequency (85-400 kHz) DCM/CCM boundary experimental circuit were built for the universal ac-line input (90 - 264  $V_{rms}$ ) with a 400-V output. Because of cost concerns and high light-load efficiency requirements, in both experimental circuits, the IPP60R099CS MOSFET in TO-220 package from Infineon was used as the boost switch. In addition, diodes  $D_3$  and  $D_4$  (shown in Fig. 6) were implemented with the two bottom diodes of bridge rectifier D15XB60 from Shindengen. In the CCM experimental circuit, boost diodes  $D_1$  and  $D_2$  (shown in Fig. 6) were implemented with the SDT08S60 SiC diodes from Infineon, each boost inductor ( $L_{B1} = L_{B2} = 1.08$  mH) was implemented with two 58928-A2 high-flux powder cores from Magnetics with 52 turns of AWG#16 wire, and for bulk capacitor  $C_B$ , two 470- $\mu$ F/450-Vdc aluminum capacitors were connected in parallel. In the DCM/CCM boundary experimental circuit, the ISL9R860P2 fast-recovery diodes from Fairchild were used as boost diodes  $D_1$  and  $D_2$ , each boost inductor ( $L_{B1} = L_{B2} = 85$   $\mu$ H) was implemented with the PQ26/25-3C96 ferrite cores from Ferroxcube with 25 turns of 0.1x80 Litz wire, and for bulk capacitor  $C_B$ , one 270- $\mu$ F/450-Vdc aluminum capacitor was used.

The control circuit of the CCM implementation is based on the ICE1PCS01 controller IC from Infineon, whereas, the control circuit of the DCM/CCM boundary implementation is based on a controller ASIC similar to the NCP1601 controller IC from ON Semiconductor. Both control circuits are very simple because the controller ICs do not require the detection of the positive and negative half cycles of the line voltage. The two boost switches are simultaneously driven with the same gate drive signal from the corresponding controller IC. For current sensing, current transformers were used.

To compare the performance of the bridgeless and conventional PFC boost rectifiers, the same prototype hardware was used. In the conventional PFC rectifier, boost switch  $S_B$  in Fig. 2 was implemented with the two boost switches  $S_1$  and  $S_2$  in Fig. 6 connected in parallel, and boost diode  $D_B$  in Fig. 2 was implemented with the two boost diodes  $D_1$  and  $D_2$  in Fig. 6 connected in parallel. For boost inductor  $L_B$  in Fig. 2, only one boost inductor  $L_{B1}/L_{B2}$  in Fig. 6 was employed. Finally, as full-bridge rectifier,  $D_1$ - $D_4$  in Fig. 2, the D15XB60 bridge rectifier from Shindengen was used.

Efficiency measurements are presented in Figs. 11 and 12. It can be seen in Fig. 11 that the CCM bridgeless PFC boost rectifier exhibits an improved efficiency of 1-2% at output power levels 350-750 W, around 3.5% at 150-W (20% load), and over 7% at 50-W output power at worst case (low line) compared to its conventional CCM counterpart. It follows from Fig. 12 that the DCM/CCM boundary bridgeless PFC boost rectifier improves the worst-case efficiency (low line) by 0.8% at full load and by almost 5% at 60-W (20% load) compared to its conventional DCM/CCM counterpart.

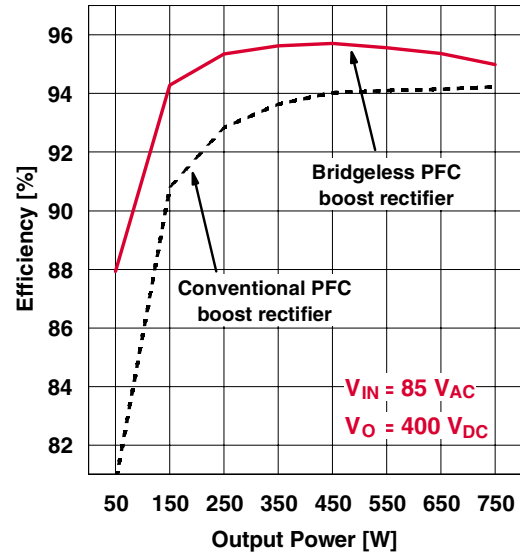


Fig. 11 Measured efficiency of conventional PFC boost rectifier in Fig. 2 (dashed line) and bridgeless PFC boost rectifier in Fig. 6 (solid line) operating in CCM

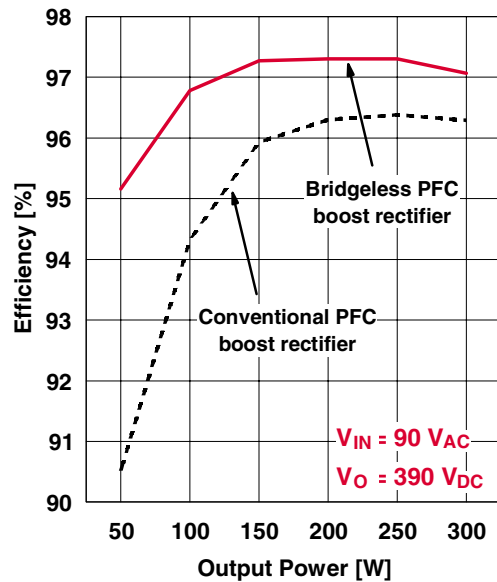


Fig. 12 Measured efficiency of conventional PFC boost rectifier in Fig. 2 (dashed line) and bridgeless PFC boost rectifier in Fig. 6 (solid line) operating at DCM/CCM boundary

It can be concluded from Figs. 11 and 12 that the DCM/CCM boundary implementation of the bridgeless PFC boost rectifier has a slightly better efficiency than the CCM implementation.

Measured line voltage and line current waveforms of the bridgeless PFC boost rectifier in Fig. 6 at full load, at low line and high line are respectively shown in Figs. 13 and 14 for the CCM implementation and in Figs. 15 and 16 for the DCM/CCM boundary implementation. It follows from Figs. 13-16 that the quality of the line current in CCM implementation is slightly better than that in the DCM/CCM boundary implementation, especially at high line. The distortion in the line current waveform in the DCM/CCM boundary implementation is caused by the non-uniform valley switching of the MOSFETs. Nevertheless, the line current in the DCM/CCM boundary implementation still meets the standards for the line current harmonics such as EN 61000-3-2. The measured PF and THD at full load and low line are 99.9% and 3.5% for the CCM implementation and 99.5% and 7.4% for the DCM/CCM boundary implementation. The measured PF and THD at full load and high line are 99.1% and 7.9% for the CCM implementation and 90.9% and 25.1% for the DCM/CCM boundary implementation.

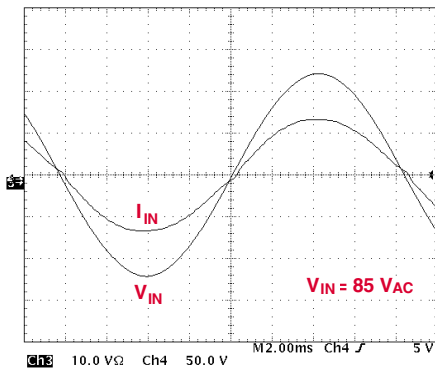


Fig. 13 Measured line voltage and line current waveforms of bridgeless PFC boost rectifier in Fig. 6 operating in CCM at full load (750 W) at 85-Vrms line voltage (PF = 99.9%, THD = 3.5%)

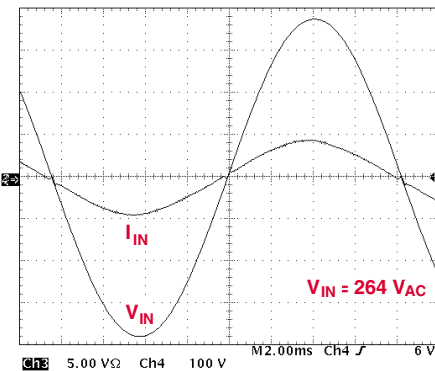


Fig. 14 Measured line voltage and line current waveforms of bridgeless PFC boost rectifier in Fig. 6 operating in CCM at full load (750 W) at 264-Vrms line voltage (PF = 99.1%, THD = 7.9%)

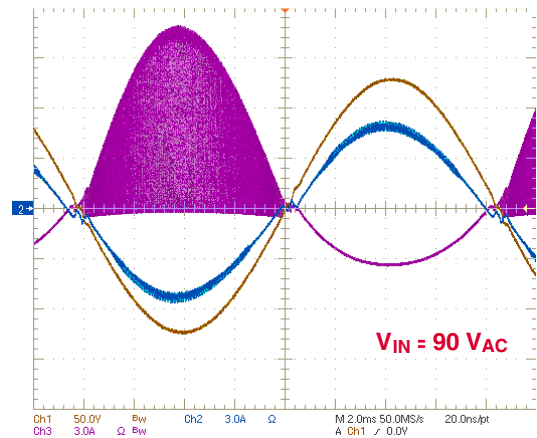


Fig. 15 Measured line voltage (Ch1), line current (Ch2), and boost-inductor current (Ch3) waveforms of bridgeless PFC boost rectifier in Fig. 6 operating at DCM/CCM boundary at full load (300 W) at 90-Vrms line voltage (PF = 99.5%, THD = 7.4%)

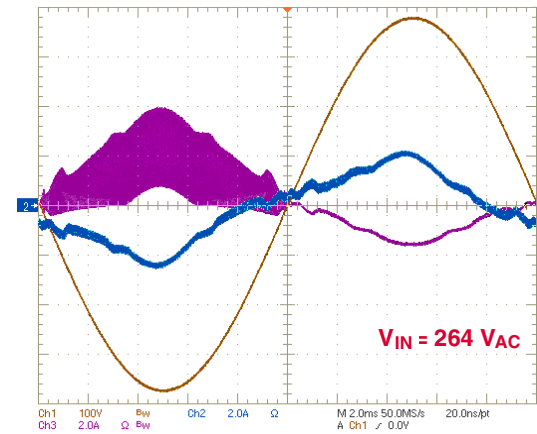


Fig. 16 Measured line voltage (Ch1), line current (Ch2), and boost-inductor current (Ch3) waveforms of bridgeless PFC boost rectifier in Fig. 6 operating at DCM/CCM boundary at full load (300 W) at 264-Vrms line voltage (PF = 90.9%, THD = 25.1%)

Figures 15 and 16 include also the measured boost-inductor current waveform. The switching frequency variation at full load, low line and high line is 85-130 kHz and 60-400 kHz, respectively. As shown in Fig. 16, at full load and high line, around the peak value of the line voltage, the boost inductor slightly enters the CCM operation, which is the result of the limitation of the controller IC.

It should be noted in Figs. 15 and 16 that the boost-inductor current during the corresponding idle half line cycle is not zero. In fact, the line-frequency component of the return current of the active boost inductor (e.g.,  $L_{B1}$  during a positive half-line cycle in Fig. 6) flows not only through the return diode but also through the non-active boost switch and the non-active boost inductor (e.g.,  $D_4$  and  $S_2-L_{B2}$  during a positive half-line cycle in Fig. 6) depending on the impedances of the two available current paths.

## V. SUMMARY

The bridgeless PFC boost rectifiers, also called the dual boost PFC rectifiers, compared to the conventional PFC boost rectifier, generally, improve the efficiency of the front-end PFC stage by eliminating one diode forward-voltage drop in the line-current path. The basic bridgeless PFC boost rectifier [1] is not a practical solution because it has significantly larger common-mode noise than the conventional PFC boost rectifier. Today, two topologies can be considered as attractive for practical implementation: the bridgeless PFC boost rectifier with the bidirectional switch [3] and the bridgeless PFC boost rectifier with two dc/dc boost circuits [10]. In this paper, the bridgeless PFC boost rectifier with two dc/dc boost circuits is selected as a representative member of the bridgeless PFC boost rectifier family for performance comparison with the conventional PFC boost rectifier.

A 750-W, constant switching frequency (110 kHz) CCM experimental circuit and a 300-W, variable switching frequency (85-400 kHz) DCM/CCM boundary experimental circuit were built for the universal ac-line input (90 - 264  $V_{\text{rms}}$ ) with a 400-V output.

The CCM bridgeless PFC boost rectifier had an improved efficiency of 1-2% at output power levels 350-750 W and around 3.5% at 20% load, whereas, the DCM/CCM boundary bridgeless PFC boost rectifier improved the efficiency by 0.8% at full load and by almost 5% at 20% load at worst case (low line) compared to their respective conventional CCM and DCM/CCM boundary counterparts. It was found that the DCM/CCM boundary implementation had a slightly better efficiency than the CCM implementation. However, the quality of the line current in the CCM implementation was slightly better than that in the DCM/CCM boundary implementation, especially at high line.

## REFERENCES

- [1] D.M. Mitchell, "AC-DC Converter having an improved power factor", U.S. Patent 4,412,277, Oct. 25, 1983.
- [2] J.C. Salmon, "Circuit topologies for single-phase voltage-doubler boost rectifiers," *IEEE Applied Power Electronics (APEC) Conf. Proc.*, pp. 549-556, Mar. 1992.
- [3] D. Tollik and A. Pietkiewicz "Comparative analysis of 1-phase active power factor correction topologies," *International Telecommunication Energy Conf. (INTELEC) Proc.*, pp. 517-523, Oct. 1992.
- [4] P.N. Enjeti and R. Martinez, "A high performance single phase AC to DC rectifier with input power factor correction," *IEEE Applied Power Electronics (APEC) Conf. Proc.*, pp. 190-195, Mar. 1993.
- [5] A.F. Souza and I. Barbi, "A new ZVS-PWM unity power factor rectifier with reduced conduction losses," *IEEE Trans. Power Electronics*, vol. 10, No. 6, pp. 746-752, Nov. 1995.
- [6] A.F. Souza and I. Barbi, "A new ZVS semiresonant high power factor rectifier with reduced conduction losses," *IEEE Trans. Industrial Electronics*, vol. 46, No. 1, pp. 82-90, Feb. 1999.
- [7] U. Moriconi, "A bridgeless PFC configuration based on L4981 PFC controller," Application Note AN 1606, STMicroelectronics, 1/18-18/18, Nov. 2002.
- [8] C.M. Wang, "A novel zero-voltage switching PWM boost rectifier with high power factor and low conduction losses," *International Telecommunication Energy Conf. (INTELEC) Proc.*, pp. 224-229, Oct. 2003.
- [9] J.C. Salmon, "Circuit topologies for PWM boost rectifiers operated from 1-phase and 3-phase ac supplies and using either single or split dc rail voltage outputs," *IEEE Applied Power Electronics (APEC) Conf. Proc.*, pp. 473-479, Mar. 1995.
- [10] A.F. Souza and I. Barbi, "High power factor rectifier with reduced conduction and commutation losses," *International Telecommunication Energy Conf. (INTELEC) Proc.*, Session 8, Paper 1, Jun. 1999.
- [11] T. Ernő and M. Frisch, "Second generation of PFC solutions," *Power Electronics Europe, Issue 7*, pp. 33-35, 2004.
- [12] J. Liu, W. Chen, J. Zhang, D. Xu, and F.C. Lee, "Evaluation of power losses in different CCM mode single-phase boost PFC converters via simulation tool," *IEEE Industry Applications Conf. (IAS) Record*, Session: High frequency power conversion, Paper 4, Sep. 2001.
- [13] H. Ye, Z. Yang, J. Dai, C. Yan, X. Xin, and J. Ying, "Common mode noise modeling and analysis of dual boost PFC circuit," *International Telecommunication Energy Conf. (INTELEC) Proc.*, pp. 575-582, Sep. 2004.
- [14] B. Lu, R. Brown, and M. Soldano, "Bridgeless PFC implementation using one cycle control technique," *IEEE Applied Power Electronics (APEC) Conf. Proc.*, pp. 812-817, Mar. 2005.
- [15] P. Kong, S. Wang, and F.C. Lee, "Common mode EMI noise suppression in bridgeless boost PFC converter," *CPES Power Electronics Conf. Proc.*, pp. 65-70, Apr. 2006.